Cycloaddition Reactions of the Phosphinidene-Bridged Complex $[Mo_2Cp(\mu\text{-}\kappa^1\!:\!\kappa^1,\eta^5\text{-}PC_5H_4)(CO)_2(\eta^6\text{-}HMes^*)]$ with Diazoalkanes and other Heterocumulenes

Isabel G. Albuerne, M. Angeles Alvarez, Inmaculada Amor, M. Esther García,* Daniel García-Vivó, and Miguel A. Ruiz*

Departamento de Química Orgánica e Inorgánica/IUQOEM, Universidad de Oviedo, E-33071 Oviedo, Spain.

Abstract

The title phosphinidene complex reacted at room temperature with CS_2 and SCNPh to give the phosphanyl derivatives $[Mo_2Cp\{\mu\text{-}\kappa^2_{P,S}\!:\!\kappa^1_{S'},\eta^5\text{-}P(CS_2)C_5H_4\}(CO)_2(\eta^6\text{-}HMes^*)]$ and $[Mo_2Cp\{\mu\text{-}\kappa^2_{P,S}\!:\!\kappa^1_{P},\eta^5\text{-}P(C(NPh)S)C_5H_4\}(CO)_2(\eta^6\text{-}HMes^*)]$ respectively (Mes* = 2,4,6-$C_6H_2{}^tBu_3$), which result from a [2+2] cycloaddition of a C=S bond in the organic reagent to the Mo=P bond of the phosphinidene complex, with further insertion of S into the remaining Mo–P bond, in the CS_2 reaction. The title complex also reacted with diazoalkanes N_2CRR' at room temperature to give the corresponding phosphaalkene derivatives $[Mo_2Cp\{\mu\text{-}\eta^2\!:\!\kappa^1_{P},\eta^5\text{-}P(CRR')C_5H_4\}(CO)_2(\eta^6\text{-}HMes^*)]$, [CRR´= CH_2, CPh_2, $CH(SiMe_3)$]. These products follow from a formal [2+1] cycloaddition of the carbene CRR´ fragment to the Mo=P bond of the parent compound, but were shown to proceed through a [3+2] cycloaddition of the diazoalkane molecule, followed by N_2 elimination. The diazomethane reaction allowed the identification at low temperature of a stabilized form of the intermediate product, the phosphanyl complex $[Mo_2Cp\{\mu\text{-}\kappa^2_{P,N}\!:\!\kappa^1_{P},\eta^5\text{-}P(CHN_2H)C_5H_4\}(CO)_2(\eta^6\text{-}HMes^*)]$, which follows from a reversible 1,3-shift of a methylenic H atom from C to N. It was concluded that all the above cycloaddition reactions are initiated by heteroatom coordination of the unsaturated organic molecule to the $MoCp(CO)_2$ fragment in the parent phosphinidene complex, this triggering the P–C bond formation step which leads to the products eventually isolated. The structures of the new complexes were determined by spectroscopic, diffractometric and, in some cases, density functional theory methods.

Introduction

The chemistry of transition-metal complexes bearing the versatile phosphinidene ligand (PR) remains an active area of research still having substantial room for

unexpected results and unusual features.[1] Most of the previous work in this field has been carried out by using mononuclear complexes, particularly those displaying bent-terminal ligands (**B** and **C** in Chart 1), which are very reactive towards a great variety of saturated and unsaturated organic molecules, whereby a large number of unusual organophosphorus molecules can be built on.[2,3] Classical examples of this chemistry are the reactions of electrophilic complexes of type **B** with alkynes to give phosphirene derivatives, or those of nucleophilic complexes of type **C** with ketones to give phosphaalkenes (the so-called phospha-Wittig reaction). The chemistry of binuclear phosphinidene-bridged complexes has been far less explored, however this situation has been changing in the last years. The electronic features of the PR ligand in its three known coordination modes (**D** to **F**), which differ in the presence of either a lone electron pair at the P site or M–P multiple bonding, should allow them to react easily with a large variety of unsaturated organic molecules. Studies involving complexes with pyramidal phosphinidene bridges of type **F** are limited to those devoted to reactions of the diiron complexes $[Fe_2Cp_2(\mu\text{-PR})(\mu\text{-CO})(CO)_2]$ (Cy, Ph, Mes, Mes*) with alkenes, alkynes, diazoalkanes, azides and quinones,[4] and those of the dimolybdenum complex $[Mo_2Cp(\mu\text{-}\kappa^1\text{:}\kappa^1,\eta^5\text{-}PC_5H_4)(CO)_2(\eta^6\text{-HMes*})(PMe_3)]$ with maleic anhydride (Mes* = 2,4,6-$C_6H_2{}^tBu_3$).[5] These reactions invariably involve initial nucleophilic attack of the phosphinidene P atom to the unsaturated organic molecule, with formation of new P–C or P–N bonds, sometimes followed by interesting rearrangements. Concerning complexes with symmetric trigonal phosphinidene bridges of type **D**, we note the extensive studies carried out on reactions of the ditungsten complex $[W_2(\mu\text{-PCp*})(CO)_{10}]$ (Cp* = C_5Me_5) with alkynes, phosphaalkynes, nitriles, isocyanides, carbodiimides, azides and carboimidophosphenes.[6] These are generally quite complex processes often involving the active participation of the Cp* ring but still yielding very unusual and remarkable organophosphorus ligands. Besides, the scandium complex $[Sc_2(\mu\text{-PXyl})_2L_2]$ (L_2= bidentate diiminate ligand) has been shown to undergo easy cycloaddition and insertion reactions with unsaturated molecules such as allenes, CS_2, nitriles and isocyanides, with selective formation of P–C bonds, while being also able to fully cleave the carbon monoxide molecule.[1c] Similar processes operate in reactions of the aminophosphinidene complexes $[Mn_2\{\mu\text{-P}(N^iPr_2)\}(CO)_8]$ and $[Co_2\{\mu\text{-P}(N^iPr_2)\}(CO)_4(\mu\text{-}Ph_2PCH_2PPh_2)]$ with diazoalkanes and azides, although P–N bond formation takes place preferentially here.[7] In contrast, some neodymium and lutetium complexes with trigonal phosphinidene bridges display phospha-Wittig behavior in reactions with aldehydes and ketones,[8] reminiscent of the chemical behavior of nucleophilic mononuclear complexes.

Chart 1

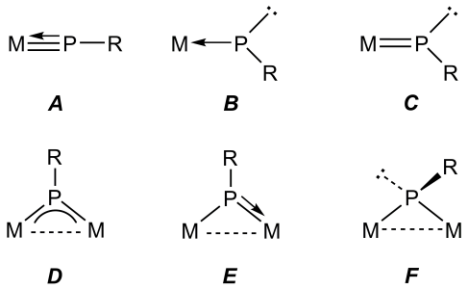

The reactions of asymmetric trigonal phosphinidene complexes of type **E** toward unsaturated organic molecules remain largely unexplored. Actually, the unique studies in this respect involve reactions of the cyclopentadienylidene-phosphinidene complex $[Mo_2Cp(\mu\text{-}\kappa^1\text{:}\kappa^1,\eta^5\text{-}PC_5H_4)(CO)_2(\eta^6\text{-}HMes^*)]$ (**1**) with alkenes and alkynes, which are much accelerated by the presence of additional ligands such as CO or isocyanides.[9] These reactions invariably involve the multiple Mo–P bond of **1** and eventually yield cycloaddition products containing four- and five-membered phosphametallacycles ($MoPC_2$ and $MoPC_3$ rings), but are initiated by coordination of a ligand (alkyne, CO, CNR) to the $MoCp(CO)_2$ fragment of the parent substrate, to yield pyramidal phosphinidene intermediates of type **F** which effectively initiate the nucleophilic attack of the P atom to the unsaturated hydrocarbon. Here we report our studies on the reactivity of **1** towards other unsaturated organic molecules, particularly some heterocumulenes displaying C–N and C–S double bonds, as it is the case of diazoalkanes, CS_2 and isothiocyanates. As it will be shown, all these reactions involve cycloaddition of the organic molecule to the double Mo–P bond of **1**, with selective formation of P–C bonds, which might be followed by additional processes, including an unexpected and reversible 1,3-H shift in the case of the diazomethane derivative.

Results and Discussion

Reactions of 1 with CS_2 and SCNPh. Although compound **1** does not react with CO_2 (ca. 4 atm) even upon moderate heating (toluene, 363 K), it does react smoothly with CS_2 at room temperature to give the phosphanyl derivative $[Mo_2Cp\{\mu\text{-}\kappa^2_{P,S}\text{:}\kappa^1_{S'},\eta^5\text{-}P(CS_2)C_5H_4\}(CO)_2(\eta^6\text{-}HMes^*)]$ (**2**) in good yield. In a related way, **1** failed to react with *p*-tolylisocyanate even in toluene solution at 363 K, but reacts with phenylisothiocyanate at room temperature to give the related derivative $[Mo_2Cp\{\mu\text{-}\kappa^2_{P,S}\text{:}\kappa^1_{P},\eta^5\text{-}P(C(NPh)S)C_5H_4\}(CO)_2(\eta^6\text{-}HMes^*)]$ (**3**) in good yield (Scheme 1).

Scheme 1

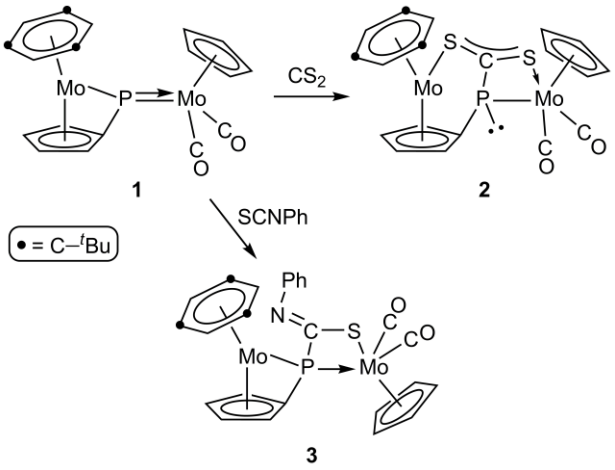

Compounds **2** and **3** formally follow from a [2+2] cycloaddition of a C=S bond of the organic reagent to the Mo=P bond present in the parent complex, with specific formation of a P–C bond. In the CS_2 reaction, there is a further coordination of the remaining S atom which cleaves the Mo–P bond to the metallocene fragment. The bridging ligand in this product is a phosphinidene-carbon disulphide adduct ($RP–CS_2$) of which we can quote only one precedent, recently prepared from the mentioned phosphinidene complex $[Sc_2(\mu\text{-}PXyl)_2L_2]$ and CS_2,[1c] although the coordination mode of the multidentate ligand in this scandium complex (μ-*P*,*S*:*S*,*S*) is slightly different from that in **2** (μ-*P*,*S*:*S*, excluding the coordination of the C_5 ring). The bridging ligand in complex **3** is a phosphinidene-isothiocyanate adduct (RP–C(S)NR) of which we can quote no previous examples. However, this ligand defines a PCSMo metallacycle completely analogous to those present in the complexes obtained in reactions of the mononuclear phosphanyl complexes $[ML(PR_2)(CO)_2]$ with different isothiocyanates (M= Mo, W; L= Cp, Cp*; R = Ph, H, ^{t}Bu).[10] These metallacyclic complexes in turn are models of the intermediates presumably formed in reactions of other mononuclear phosphanyl complexes which end up with full insertion of the added isothiocyanate into the Mo–P bond of the parent substrate.[11]

Structural Characterization of Compound 2. The molecular structure of **2** in the crystal (Figure 1 and Table 1) confirms the presence of a highly polyfunctional $RPCS_2$ ligand bridging the metal centers, *P*,*S*-bound to the Mo1 atom while bound to the Mo2 atom through the cyclopentadienylidene ring (in the usual η^5 fashion) and the second S atom of the added CS_2 molecule. The environment around the C3 atom is almost perfectly planar, thus allowing for delocalization of any π-bonding interaction, while the P atom displays a significant pyramidalyzation (Σ X–P–Y = 298.4°), thus pointing to the presence of a lone electron pair at this site. The Mo–P and Mo–S lengths of ca. 2.57 and 2.53 Å respectively are not unusual for single-bond interactions involving these atoms, nor is the P–C3 length of 1.772(2) Å (1.80 Å expected for a P–C(sp^2) bond).[12] In

contrast, both C–S lengths in **2** are similar to each other and close to 1.70 Å, a figure intermediate between the reference values for single (1.78 Å) and double bonds (1.62 Å) between these atoms,[13] which suggests full delocalization of a π bonding electron pair along the S–C–S skeleton (angle 124.8(1)°), as found in $R_3P–CS_2$ adducts and many of their metal complexes.[14]

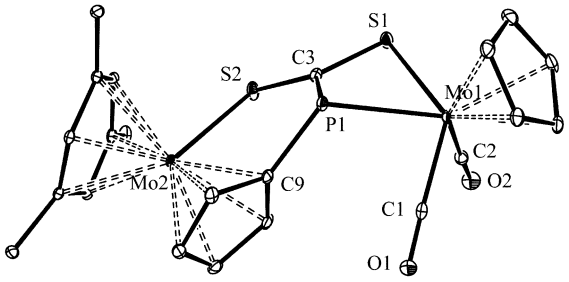

Figure 1. ORTEP diagram (30% probability) of compound **2**, with H atoms and ^{t}Bu groups (except their C^1 atoms) omitted for clarity.

Table 1. Selected Bond Lengths (Å) and Angles (°) for Compound **2.**

Mo1–P1	2.5665(5)	P1–Mo1–S1	68.39(2)
Mo1–S1	2.5240(5)	C1–Mo1–C2	77.19(8)
Mo1–C1	1.960(2)	C1–Mo1–P1	78.62(6)
Mo1–C2	1.935(2)	C2–Mo1–P1	115.69(6)
Mo2–S2	2.5406(5)	Mo1–P1–C9	118.25(6)
P1–C3	1.772(2)	Mo1–P1–C3	84.01(6)
P1–C9	1.818(2)	C3–P1–C9	96.12(9)
C3–S1	1.705(2)	P1–C3–S1	110.7(1)
C3–S2	1.692(2)	P1–C3–S2	124.0(1)
		S1–C3–S2	124.8(1)

Spectroscopic data in solution for compound **2** are consistent with the structure found in the crystal, devoid of any symmetry elements (Table 2 and Experimental section). Its ^{31}P NMR resonance appears at 18.6 ppm, some 500 ppm more shielded than that of the phosphinidene complex **1**,[15] and is consistent with the retention in solution of a pyramidal phosphanyl P atom bound to a single metal and bearing a lone electron pair.[16] For comparison, the ^{31}P chemical shift of the pyramidal phosphanyl ligand in $[MoCp(PPh_2)(CO)_2(PMe_3)]$ is –31.9 ppm.[17] Retention of the *P*,*S*-chelating coordination of the bridging ligand to the $MoCp(CO)_2$ fragment of the molecule is indicated by the inequivalence and different P-C couplings of the corresponding ^{13}C NMR carbonyl resonances (δ_C = 250.6 (s) and 248.7, $^2J_{CP}$ = 9). The CS_2 atom gives rise to a strongly deshielded and P-coupled resonance as expected (δ_C = 250.3, J_{CP} = 58).

Table 2. Selected IR[a] and $^{31}P\{^1H\}$ NMR Data[b] for New Compounds

Compound	ν(CO)	$\delta(\mu$-P)
$[Mo_2Cp(\mu\text{-}\kappa^1\!:\!\kappa^1,\eta^5\text{-}PC_5H_4)(CO)_2(\eta^6\text{-HMes*})]$ (**1**)[c]	1908 (vs), 1827 (s)	519.0
$[Mo_2Cp\{\mu\text{-}\kappa^2_{P,S}\!:\!\kappa^1_{S'},\eta^5\text{-}P(CS_2)C_5H_4\}(CO)_2(\eta^6\text{-HMes*})]$ (**2**)	1932 (vs), 1845 (s)	18.6[d]
$[Mo_2Cp\{\mu\text{-}\kappa^2_{P,S}\!:\!\kappa^1_{P},\eta^5\text{-}P(C(NPh)S)C_5H_4\}(CO)_2(\eta^6\text{-HMes*})]$ (**3**)	1946 (vs), 1865 (s)	26.4[d]
$[Mo_2Cp\{\mu\text{-}\kappa^2_{P,N}\!:\!\kappa^1_{P},\eta^5\text{-}P(CHN_2H)C_5H_4\}(CO)_2(\eta^6\text{-HMes*})]$ (**4**)	1950 (vs), 1880 (s)[e]	124.8[f]
$[Mo_2Cp\{\mu\text{-}\eta^2\!:\!\kappa^1_{P},\eta^5\text{-}P(CH_2)C_5H_4\}(CO)_2(\eta^6\text{-HMes*})]$ (**5a**)	1914 (vs), 1830 (s)[g]	67.2 (*anti*)[h] 41.9 (*syn*)[h]
$[Mo_2Cp\{\mu\text{-}\eta^2\!:\!\kappa^1_{P},\eta^5\text{-}P(CPh_2)C_5H_4\}(CO)_2(\eta^6\text{-HMes*})]$ (**5b**)	1918 (vs), 1821 (s)	63.5
$[Mo_2Cp\{\mu\text{-}\eta^2\!:\!\kappa^1_{P},\eta^5\text{-}P(CHSiMe_3)C_5H_4\}(CO)_2(\eta^6\text{-HMes*})]$ (**5c**)	1912 (vs), 1825 (s)[i]	88.2 (*anti*)[h] 70.9 (*syn*)[h]

[a] Recorded in dichloromethane solution, with C–O stretching bands [ν(CO)] in cm^{-1}. [b] Recorded in CD_2Cl_2 solution at 162.12 MHz and 298 K unless otherwise stated. [c] Data taken from reference 15. [d] In C_6D_6 solution. [e] In petroleum ether solution. [f] In toluene-d_8 solution at 233 K. [g] ν(CO) 1934 (vs), 1865 (m), 1858 (m) in petroleum ether solution. [h] Recorded at 233 K. [i] ν(CO) 1936 (vs), 1927 (s), 1855 (s), 1848 (m) in petroleum ether solution.

Structural Characterization of Compound 3. The molecular structure of **3** in the crystal (Figure 2 and Table 3) can be derived from that of **1** after formal cycloaddition of the C–S bond of the isothiocyanate molecule to the short Mo–P bond in **1** in a plane perpendicular to its Mo_2P plane, with specific formation of P–C and Mo–S bonds. As a result, the $MoCp(CO)_2$ fragment of the molecule ends up bound to a chelating *P*,*S*-donor group which eventually completes a classical four-legged piano stool geometry around the metal atom, as found also in **2**. Dimensions within the puckered MoPCS ring of **3** are comparable to those measured in the W phosphanyl derivative $[WCp^*\{\kappa^2_{P,S}\text{-}PR^tBuC(NMe)S\}(CO)_2]$,[10c] (R = C(S)NHMe), or the Re_2 phosphaalkene derivative $[Re_2\{\mu\text{-}\kappa^1_P\!:\!\kappa^2_{P,S}\text{-}P(E)C(NPh)S\}_2(CO)_6]$,[18] ($E = C(NMe_2)_2$), and are consistent with the formulation of essentially single bonds between these atoms. In contrast, the exocyclic C–N length of 1.276(4) Å corresponds to a fully localized double C–N bond (the reference value is 1.27 Å).[13] We note, however, that the Mo1–P length in **3** is ca 0.1 Å shorter than the corresponding distance in **2**, which is consistent with the absence of the repulsive action of a lone electron pair at the P atom, and the formulation of a single donor bond to the metal atom. Interestingly, the chemical environment of the P atom in **3** deviates significantly from the usual tetrahedral geometry expected for a PR_2 ligand bridging two metal atoms, since the Mo1, Mo2 and C3 atoms are almost coplanar with the P atom (Σ X–P–Y ca. 358°) while the cyclopentadienylidene C atom defines an angle of ca. 60° with that plane. This completes a distorted trigonal-pyramidal-like geometry around the P atom which we have found previously in different alkyne,[9c] chalcogen,[19] and heterometallic derivatives of compound **1**,[9a,20] a matter to be addressed below. We finally note that the C_5 rings in **3** are arranged in a *syn* conformation, in contrast to the *anti* arrangement of these rings in **1** and many of their derivatives. This is not surprising after our previous finding that the alkyne derivatives of **1**, of formula

$[Mo_2Cp\{\mu\text{-}\kappa^2_{P,C}\text{:}\kappa^1_P,\eta^5\text{-}P(CRCR')C_5H_4\}(CO)_2(\eta^6\text{-}HMes^*)]$, which are structurally related to compound **3**, display in solution *syn*/*anti* interconversion at room temperature, thus indicating low kinetic barriers and reduced thermodynamic balance for this conformational change. As discussed below, this sort of isomerism is actually present in the phosphaalkene derivatives of **1**.

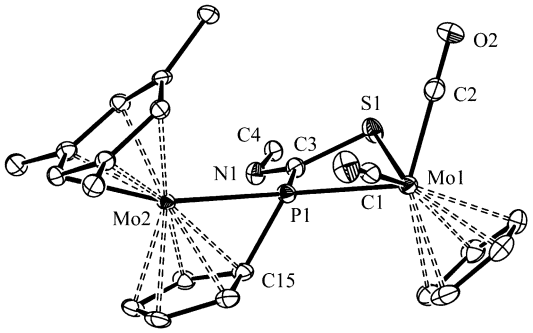

Figure 2. ORTEP diagram (30% probability) of compound **3**, with H atoms, ^{t}Bu and Ph groups (except their C^1 atoms) omitted for clarity.

Table 3. Selected Bond Lengths (Å) and Angles (º) for Compound **3.**

Mo1–P1	2.4523(8)	P1–Mo1–S1	66.76(3)
Mo1–S1	2.5274(8)	C1–Mo1–C2	77.9(1)
Mo1–C1	1.966(3)	C1–Mo1–P1	78.9(1)
Mo1–C2	1.960(3)	C2–Mo1–P1	111.0(1)
Mo2–P1	2.5296(7)	Mo1–P1–C15	121.5(1)
P1–C3	1.821(3)	Mo1–P1–C3	95.2(1)
P1–C15	1.780(3)	C3–P1–C15	110.7(1)
C3–S1	1.766(3)	P1–C3–S1	99.6(2)
C3–N1	1.276(4)	P1–C3–N1	128.5(2)
N1–C4	1.420(4)	S1–C3–N1	131.8(2)
		C3–N1–C4	118.4(3)

Spectroscopic data in solution for **3** are consistent with the structure found in the solid state. The spectroscopic properties of the $MoCp(CO)_2$ fragment are comparable to those found in **2** and deserve no further comment, and the isothiocyanate carbon atom gives rise to a P-coupled (J_{CP} = 7) and moderately deshielded NMR resonance at 190.7 ppm (cf. δ_C = 183-190 ppm, and J_{CP} = 23-30 Hz for complexes $[MCp^*\{\kappa^2_{P,S}\text{-}PR^tBuC(NR')S\}(CO)_2]$, (M = Mo, W).[10c] Compound **3** displays a quite shielded ^{31}P NMR resonance at 26.4 ppm, actually very close to that of **2** (Table 2) even if there is not a lone electron pair at the P atom in this case. Such a strong shielding, however, is a common feature for PR_2 ligands bridging metal atoms which are not connected by a direct intermetallic bond.[21]

Pathways in the Reactions of 1 with CS_2 and SCNPh. Although compounds **2** and **3** are formally derived from cycloaddition reactions of the Mo–P double bond of **1** with the double C–S bond of the added heterocumulene, it is unlikely that these reactions actually take place in a concerted way. The fact that **1** is unreactive towards related heterocumulenes having double C–O bonds (CO_2 and RNCO) points to a very active

role of the sulfur atom in these reactions. We have shown previously that the addition of ligands (CO, CNR, PR_3) to **1** takes place at the $MoCp(CO)_2$ fragment of the molecule and causes a pyramidalization at the P atom (change from coordination mode **E** to **F**) which increases dramatically its nucleophilicity towards C-based electrophiles such as alkenes, alkynes, anhydrides and alkyl halides.[5, 9b,c, 22] It is thus reasonable to assume that reactions of **1** with the heterocumulenes under discussion are initiated by coordination of the organic reagent to the $MoCp(CO)_2$ fragment *via* the S atom. This would yield a pyramidal intermediate **I1** with increased nucleophilicity at the P atom and increased electrophilicity at the C atom of the heterocumulene, which then might rapidly evolve through P–C bond formation to give the cycloaddition product **I2** (Scheme 2). DFT calculations on $[Mo_2Cp(\mu\text{-}\kappa^1\text{:}\kappa^1,\eta^5\text{-}PC_5H_4)(CO)_2(\eta^6\text{-}HMes^*)(PMe_3)]$ indicate that the lone pair at the P atom in this sort of pyramidal intermediates concentrates its maximum density in the Mo_2P plane,[22] so the new P–C bond must be formed in that plane. In the SCNPh reaction, the resulting intermediate **I2** yields compound **3** in a straightforward way, it only requiring an *anti*/*syn* rearrangement of the $MoCp(CO)_2$ fragment, which is an easy process, as noted above. In the CS_2 reaction, intermediate **I2** would further evolve through coordination of the second S atom to the metallocene fragment, with cleavage of the corresponding Mo–P bond to yield complex **2**.

Scheme 2

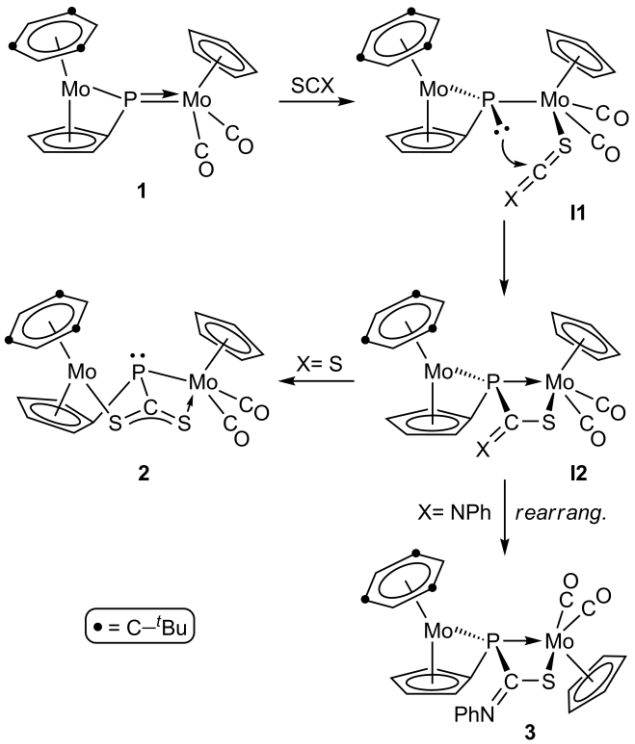

Reactions of Complex 1 with Diazoalkanes. There are only a few previous studies on the reactivity of phosphinidene complexes with diazoalkanes, but the number of

possible outputs is significant. Mononuclear electrophilic complexes of type **B** such as $[ML\{P(N^iPr_2)\}(CO)_x]^+$ (M = Fe, Cr, Mo, W; L= Cp, Cp*; x = 2, 3),[23] and $[VCp\{P(N^iPr_2)\}(CO)_3]$[24] react with N_2CPh_2 with formation of a P–N bond, to yield phosphadiazadiene ligands bound to the metal atom in κ^1, η^2 or η^3-fashions depending on the metal (**J** to **L** in Chart 2), while reaction of the iron complex with $N_2CH(SiMe_3)$ resulted in full denitrogenation to yield the corresponding *P*-bound phosphaalkene.[23] Analogously, the pyramidal phosphinidene complexes of type **F** $[Fe_2Cp_2(\mu\text{-PR})(\mu\text{-CO})(CO)_2]$ reacted with different diazoalkanes to yield μ-*P*:*P*-bridged phosphadiazadiene derivatives (**M** in Chart 2). The latter were quite resistant to denitrogenation, and upon photochemical decarbonylation just rearranged to yield products with the bridging phosphadiazadiene ligand in either *P*:*N*- or *P*:*C*- coordination modes (**N** to **Q**). Interestingly, a 1,3-$SiMe_3$ shift occurred in the photolysis of the $N_2CH(SiMe_3)$ derivative which yielded a product with an aminophosphanyl-iminoacyl bridging ligand (**R**), and denitrogenation was only observed as a side process in the photolysis of the diazomethane derivative, this leading to a μ-κ^1:η^2 bound phosphaethylene derivative.[4c] Concerning binuclear complexes with trigonal phosphinidene bridges of type **D**, we note that the dicobalt complex $[Co_2\{\mu\text{-}P(N^iPr_2)\}(CO)_4(\mu\text{-}Ph_2PCH_2PPh_2)]$ reacted with diazomethane to give the corresponding μ-κ^1:η^2 phosphaethylene derivative, whereas the dimanganese complex $[Mn_2\{\mu\text{-}P(N^iPr_2)\}(CO)_8]$ reacted with N_2CPh_2 to give a phosphadiazadiene derivative of type **N** which did not undergo denitrogenation.

Chart 2

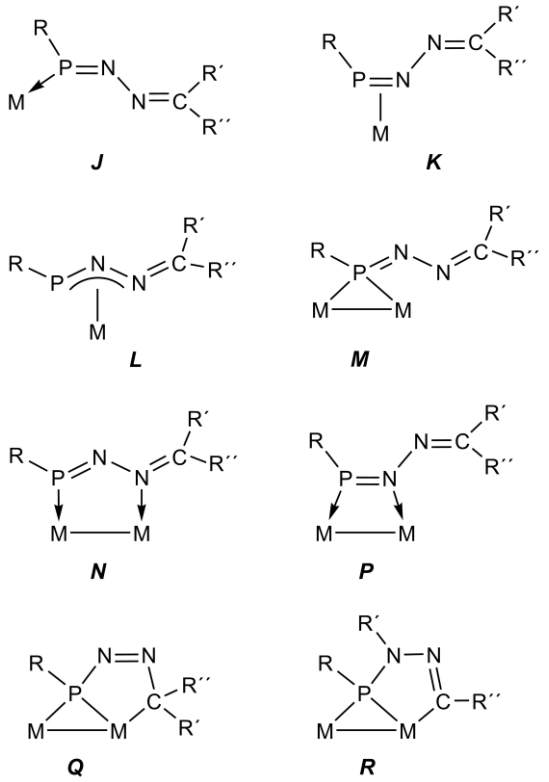

From the above precedents, it is apparent that P–N bond formation dominates the interaction with diazoalkanes of all mononuclear and binuclear phosphinidene complexes studied previously, to give products significantly resistant to denitrogenation. It was thus somewhat surprising to find that compound **1** reacted with different diazoalkanes N_2CRR' with full denitrogenation at room temperature, to give the corresponding phosphaalkene-bridged derivatives $[Mo_2Cp\{\mu\text{-}\eta^2\text{:}\kappa^1_P,\eta^5\text{-}P(CRR')C_5H_4\}(CO)_2(\eta^6\text{-HMes*})]$, [CRR´= CH_2(**5a**), CPh_2(**5b**), $CHSiMe_3$(**5c**)] in good yields (Scheme 3). The diazomethane reaction was very fast at room temperature, so we could examine it at lower temperature. Indeed, compound **1** reacts rapidly with N_2CH_2 even at 203 K, but this now gives the phosphanyl derivative $[Mo_2Cp\{\mu\text{-}\kappa^2_{P,N}\text{:}\kappa^1_P,\eta^5\text{-}P(CHN_2H)C_5H_4\}(CO)_2(\eta^6\text{-HMes*})]$ (**4**) as major product. Compound **4**, however, is thermally unstable and evolves rapidly at room temperature with full denitrogenation to yield the phosphaethylene derivative **5a** as sole product. The formation of **4** implies the operation at this substrate of a fast and reversible 1,3-H shift which is largely unprecedented, a matter to be further discussed below.

Scheme 3

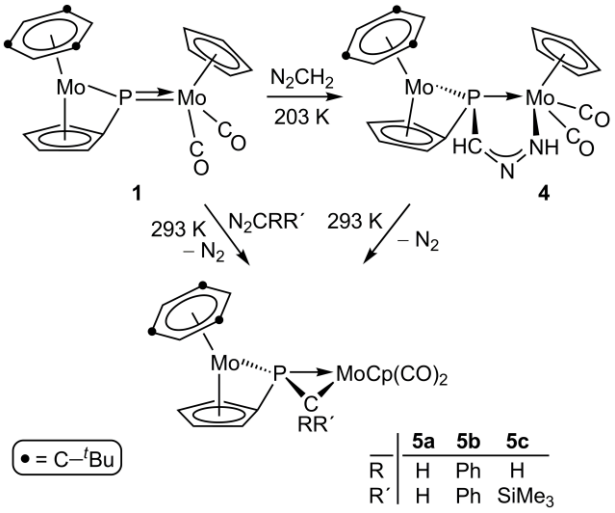

Solution Structure of Compound 4. Spectroscopic data for **4** (Table 2 and Experimental section) suggest the incorporation of a diazomethane molecule with rearrangement of their H atoms to place them apart from each other. The latter is indicated by the presence of ^{1}H NMR resonances at 6.38 and 6.26 ppm which display no mutual coupling. As indicated by a standard HSQC NMR experiment, the most deshielded resonance corresponds to a proton bound to a substantially deshielded C atom (δ_C 124.0 ppm), which suggests a sp^2 hybridization at the latter atom, while the position and negligible H–P coupling of the second resonance is compatible with a N-bound H atom. On the other hand, both the strong H–P coupling of the 6.38 ppm resonance (32 Hz) and the observation of positive NOE enhancements with the HMes* and one of the C_5H_4 protons, but not with the Cp protons, indicates that the CH group is

spatially close to the metallocene fragment of **4**, therefore bound to the P atom. In all, these data are indicative of the formation of a five-membered ring similar to those present in the mentioned Fe_2 complexes of type **R**,[4c] but following from the formation of a P–C bond, rather than a P–N one.

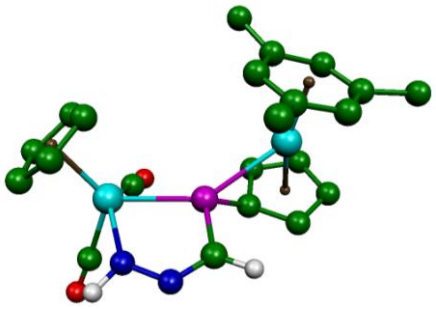

Figure 3. DFT-optimized structure for compound **4**, with most H atoms omitted for clarity. Selected distances within the ring (Å): Mo–P = 2.542; Mo–N = 2.190; P–C = 1.814; C–N = 1.298; N–N = 1.323. Exocyclic distances: P–Mo = 2.656; P–C = 1.798.

Since the low thermal stability of **4** precluded the growth of X-ray quality crystals of this compound, we resorted to density functional theory (DFT) calculations to further support our structural proposal for this complex (see the Experimental section and Supporting Information for further details). Indeed we found that such structure is a true minimum in the potential energy surface of **4** (Figure 3), with a Gibbs free energy some 5 kJ/mol below the starting materials (**1** + N_2CH_2) in the gas phase at 298 K, which makes it thermodynamically viable. Interestingly, an alternative isomer of **4** with P–N and C–Mo bonds was computed to be some 20 kJ/mol less stable, therefore thermodynamically unviable. The Mo–P, Mo–N and Mo–C lengths within the ring of **4** have values consistent with the presence of single bonds between these metal atoms. However, the C–N length of 1.298 Å is somewhat longer than the reference C=N value of 1.27 Å, whereas the N–N length of 1.323 Å is significantly shorter than the expected figure for a single bond (1.44 Å). This points to an extensive delocalization of a π bonding interaction over the N–N–C skeleton of the planar five-membered ring of this complex which could be represented by a combination of the canonical forms ***I*** and ***II*** (Figure 4). For comparison, the interatomic distances in the related diiron complex of type **R** [$Fe_2Cp_2\{\mu$-CyPN($SiMe_3$)N=CH$\}(\mu$-CO$)(CO)_2$] which, however, displays almost fully localized C=N and N–N bonds within the corresponding ring, are 1.284(5) and 1.437(5) Å respectively.[4b]

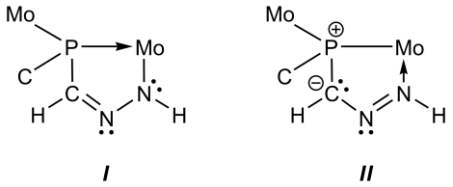

I ***II***

Figure 4. Canonical forms describing the π-bonding delocalization in the 5-membered ring of compound **4**.

Solid-State and Solution Structure of the Phosphalkene Complexes 5. The structure of the methylene (**5a**) and diphenylcarbene (**5b**) derivatives of **1** has been determined through single-crystal X-ray diffraction studies. Both structures are similar to each other (Figure 5 and Table 4) and are formally derived from the [2+1] cycloaddition of a carbene group to the Mo–P double bond of **1** perpendicular to the Mo_2P plane in the latter, where the frontier orbitals of this substrate are directed.[9a,20] The interaction pattern is thus analogous to that of **1** with chalcogen atoms,[19] and with 16-electron $M(CO)_x$ fragments,[20] as expected, and yields a phosphaalkene ligand bridging the metal atoms in a μ-κ^1:η^2 fashion. This is a relatively uncommon coordination mode of the very versatile phosphaalkene ligands,[25] and has been crystallographically characterized in a reduced number of cases.[7,26] In all reported examples, however, the phosphaalkene ligand bridges metal fragments with identical electron counts, thus formally providing 2 electrons to each of them (**X** in Figure 6). As a result, the Mo–P bond involving the σ interaction expectedly is somewhat shorter than the one involving the π interaction (e.g. 2.346 and 2.435 Å in [Mo_2Cp_2(μ-PhP=CHMe)$(CO)_4$]).[26b] We also note that the experimental P–C distances in all these complexes are found in the range 1.74-1.75 Å, indicating the retention of some multiplicity at this bond. In contrast, the electron requirements of the metal fragments in compounds **5** are different from each other, and the cycloaddition processes renders an electron distribution fitting the distinct electron demands of the metal centers (1 and 3 electrons) in a natural way (**Y** in Figure 6). As a result, the M–P length within the MPC ring is expected to be *shorter* than the exocylic M–P length, and the P–C distance should approach the reference single-bond value of 1.80 Å for a P–C(sp^2) bond. This is indeed the case of compounds **5a,b**, with endocyclic Mo–P lengths of ca. 2.40 Å and exocyclic Mo–P lengths of ca. 2.50-2.60 Å. We note that both distances are significantly longer for the CPh_2 derivative **5b**, which possibly reflects the higher steric constraints in this molecule. We also note that the endocylcic Mo1C3 length for **5b** is some 0.08 Å longer than the corresponding length in **5a**, possibly for the same reasons. In contrast, the endocyclic P–C length in both compounds is very similar, around 1.77 Å, and approaches the single-bond figure.

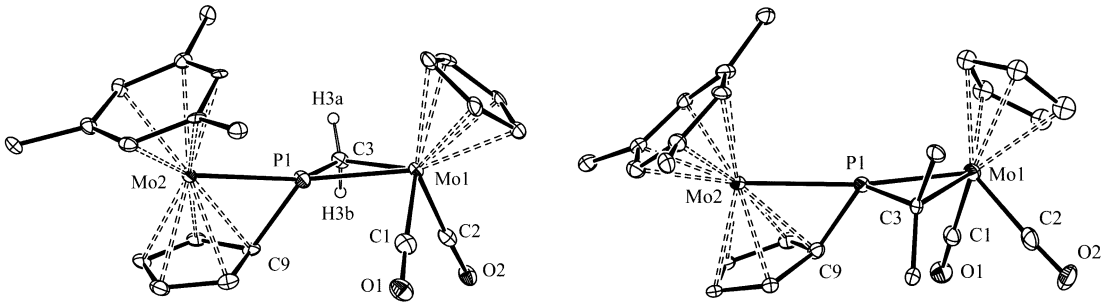

Figure 5. ORTEP diagram (30% probability) of compounds **5a** (left) and **5b** (right), with ^{t}Bu and Ph groups (except their C^1 atoms) and most H atoms omitted for clarity.

Table 4. Selected Bond Lengths (Å) and Angles (º) for Compounds **5a** and **5b.**

	5a	**5b**
Mo(1)–P(1)	2.369(3)	2.413(2)
Mo(2)–P(1)	2.480(3)	2.600(2)
Mo(1)–C(1)	1.962(12)	1.918(7)
Mo(1)–C(2)	1.929(12)	1.968(8)
Mo(1)–C(3)	2.299(11)	2.383(6)
P(1)–C(3)	1.766(11)	1.775(7)
P(1)–C(9)	1.786(10)	1.776(6)
Mo(1)–P(1)–Mo(2)	152.4(1)	159.8(1)
Mo(1)–P(1)–C(3)	65.7(4)	67.4(2)
Mo(1)–P(1)–C(9)	131.2(4)	121.8(2)
C(3)–P(1)–Mo(2)	138.1(4)	132.8(2)
C(3)–P(1)–C(9)	114.2(5)	112.0(3)
Mo(1)–C(3)–P(1)	69.9(4)	69.2(2)
C(1)–Mo(1)–C(2)	83.2(4)	83.6(3)
C(1)–Mo(1)–C(3)	117.0(4)	104.1(2)
C(2)–Mo(1)–C(3)	83.5(4)	76.6(3)

The coordination environment around the P atom in compounds **5a,b**, with the P atom placed almost in the Mo_2C3 plane, corresponds to the distorted trigonal pyramidal environment also found for **3** and different alkyne,[9c] chalcogen,[19] and heterometallic derivatives of compound **1**,[9a,20] as noticed above. We have previously attributed this unusual geometry to the geometrical constraints imposed by the bifunctional PC_5H_4 ligand combined with steric effects induced by the bulky η^6-HMes* ligand. The structural data for compounds **5** reinforce this interpretation, since the P atom reaches the Mo_2C3 plane for the complex with higher steric constrains (Σ X–P–Y angles are 356.2º for **5a** but 360.0º for **5b**).

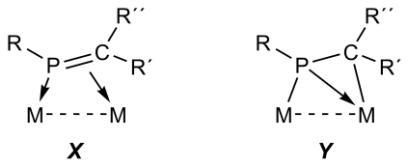

Figure 6. Extreme electron distributions in μ-κ^1:η^2-phosphaalkene ligands.

Spectroscopic data in solution for compounds **5** are consistent with the solid-state structures discussed above, but reveal the presence of two interconverting conformers for the less congested complexes **5a,c**, which would differ in the relative positioning of the C_5 rings of these molecules with respect to the Mo_2C ring (*syn* and *anti* in Scheme 4); presumably, the most congested CPh_2 derivative **5b** retains in solution the *anti* conformation found in the crystal. Thus, while the IR spectra of all these compounds in dichloromethane solution display two C–O stretching bands with relative intensities (very strong and strong, in order of decreasing frequency) consistent with the presence of cisoid $M(CO)_2$ oscillators in each case,[27] a splitting into a total of three (**5a**) or four (**5c**) bands is observed when recording the IR spectra in petroleum ether solution. In agreement with this, the ^{31}P NMR spectrum of **5c** in CD_2Cl_2 solution displays two broad resonances at room temperature which sharpen on lowering the temperature (δ_P 67.2

and 41.9 ppm at 233 K). In the case of **5a**, no ^{31}P NMR resonance is observed at room temperature, but two resonances with progressive sharpening appear on lowering the temperature (δ_P 88.2 and 70.9 ppm at 233 K). In both cases, the most deshielded resonance corresponds to the most abundant species, which is assumed to be the *anti* conformer found in the solid state, based on steric grounds. In any case, the above experimental data indicate a similar energy for these conformers in solution, in agreement with the gas-phase Gibbs free energies of these isomers in **5a**, computed to be within 0.5 kJ/mol from each other (see the SI). We recall here that similar isomerism has been previously found in alkyne,[9c] and chalcogen[19] derivatives of compound **1**. Yet we note that further isomerism would be still possible for compound **5c** depending on the relative orientation of the $SiMe_3$ group with respect to the bulky η^6-HMes* ring, but only one is observed, presumably the one having these bulky groups far apart from each other.

Scheme 4

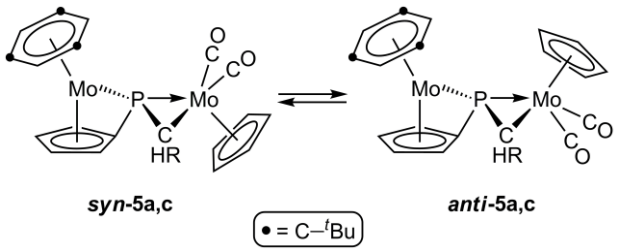

The ^{13}C NMR resonances of the methylenic carbon atom in the different isomers of compounds **5a**,**c** are found in the range $-17.1 > \delta_C > -29.1$ ppm, with a C–H coupling of 134 Hz in the case of **5c**, and the corresponding ^{1}H NMR resonances are quite shielded too ($+0.54 > \delta_H > -0.66$ ppm). All of this is indicative of an essentially sp^3 character for these methylenic C atoms, derived from the very strong coordination of the phosphaalkene ligand to the 15-electron $MoCp(CO)_2$ fragment in these complexes. We note that the above ^{13}C shieldings are substantially higher than those reported for the type **X** phosphaalkene complexes $[Mo_2Cp_2\{\mu\text{-}\kappa^1\text{:}\eta^2\text{-}P(Ph)=(CHMe)\}(CO)_4]$ (δ_C = 42 ppm),[26b] and $[Co_2Cp_2\{\mu\text{-}\kappa^1\text{:}\eta^2\text{-}P(N^iPr_2)=CH_2\}(CO)_4(\mu\text{-}Ph_2PCH_2PPh_2)]$ (δ_C = 24 ppm),[7] in agreement with the electronic differences implied by the extreme descriptions **X** and **Y** of $\mu\text{-}\kappa^1\text{:}\eta^2$ phosphaalkenes. The corresponding resonance in the CPh_2 derivative **5b** appears substantially more deshielded (δ_C= 128.3 ppm), in part due to the presence of the Ph substituents, but surely also due to the larger separation from the Mo atom evidenced in the crystal structure of this compound.

Pathways in the Reactions of Compound 1 with Diazoalkanes. The identification of compound **4** as intermediate species in a reaction with diazomethane eventually resulting in methylene cycloaddition to the Mo–P double bond of **1** suggests that [3+2] dipolar cycloaddition of diazoalkanes might well be involved in the formation of all

phosphaalkene complexes **5a-c**. Again, as discussed for the reactions of **1** with CS_2 and SCNPh, it is unlikely that these reactions proceed in a concerted way. Instead, thanks to the good coordination properties of the diazoalkane ligands,[28] these reactions are likely initiated by *N*-coordination of the added diazoalkane to the $MoCp(CO)_2$ fragment of **1** to give a pyramidal phosphinidene intermediate **I3**. The latter would have increased nucleophilicity at the P site and increased electrophilicity at the methylenic carbon, being then well suited to undergo a P–C bond formation rearrangement that would complete the formal [3+2] cycloaddition, thus yielding a second intermediate **I4** (Scheme 5). Dissociative cleavage of the Mo–N bond in the latter intermediate would allow a thermodynamically favored process releasing N_2 and yielding the final phosphaalkene complexes **5** eventually isolated. Although we have not investigated the kinetic profile of these transformations, we have checked their thermodynamic viability by computing the gas-phase Gibbs free energies at 298 K of the diazomethane derivatives, and found that intermediate **I4** is just a little more energetic than the starting reagents (17 kJ/mol above **1** + N_2CH_2), while the release of N_2 boosts the formation of **5a** (overall ΔG = –187 kJ/mol).

Scheme 5

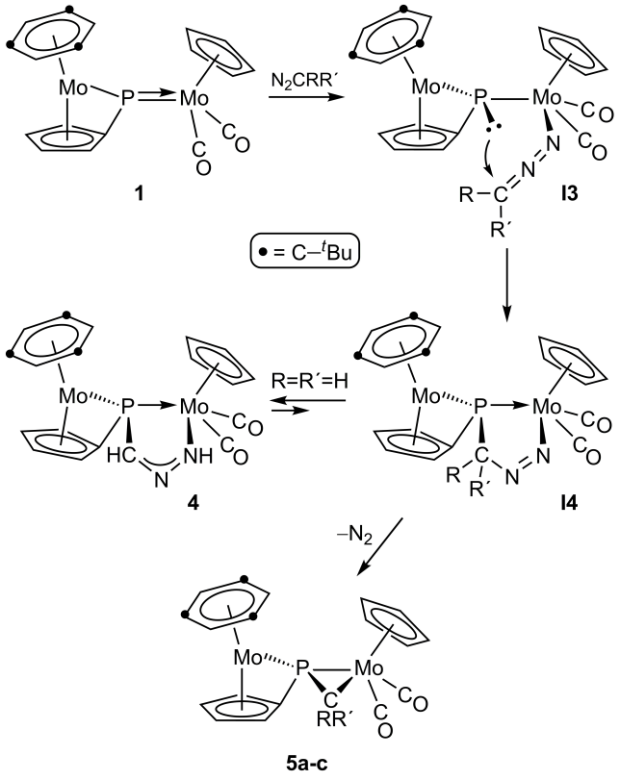

In the diazomethane reaction, however, a second pathway would be under operation, this being a 1,3-shift of a methylenic H atom up to the N atom that yields the phosphanyl complex **4** (Scheme 5). As noted above, this is a thermodynamically allowed transformation, since the Gibbs free energy of **4** is some 5 kJ/mol below the

reagents. We can quote a few precedents for this short of H shift in diazoalkanes reactions. As concerning reactions involving phosphinidene complexes, we can only quote the phosphadiazadiene complex of type **Q** [Fe_2Cp_2\{μ-CyPN=NCH(CO_2Me)\}(μ-CO)($CO)_2$], which rearranged into a derivative of type **R** [Fe_2Cp_2\{μ-CyPNHN=C(CO_2Me)\}(μ-CO)($CO)_2$] upon chromatography on alumina.[4e] An analogous rearrangement occurred in the room temperature reaction of the trigonal phosphanyl complexes [MCp(P^tBu_2)($CO)_2$] with N_2CHR to give the chelate derivatives [MCp($\kappa^2_{N,C}$-$^tBu_2$PNHN=CR)($CO)_2$], (M = Mo, W; R = CO_2Me).[29] We note that in both cases the diazoalkane molecule forms rings alike that of **4** but containing P–N bonds rather than P–C bonds, because they follow from nucleophilic attack of P to the N atom of the diazoalkane molecule. Very recently, an imine-stabilized carboranylphosphinidene has been reported to react with N_2CH(CO_2Me) to give a product requiring P–N bond formation and an 1,3-H shift in the diazoalkane fragment.[30] To our knowledge, the 1,3-H shifts in all the above examples are irreversible transformations. In contrast, such a rearrangement in **4** is a reversible process, feasible because **I4** is only 22 kJ/mol more energetic, and this eventually allows the irreversible evolution of **4** to the phosphaethylene complex **5a** and dinitrogen.

Concluding Remarks

The reactions of the phosphinidene complex **1** with the heterocumulenes CS_2, SCNPh and N_2CRR´ all proceed by heteroatom coordination of the unsaturated organic molecule to the MoCp($CO)_2$ fragment in **1** to give pyramidal phosphinidene intermediates responsible for the P–C bond formation step which completes respectively formal [2+2] and [3+2] cycloadditions of the organic substrate to the Mo=P bond in **1**, these yielding MoPCS and MoPCNN metallacycles. The cycloaddition products of diazoalkanes are thermally unstable, and evolve *via* Mo–N bond dissociation and denitrogenation to give stable phosphaalkene-bridged derivatives which display a novel coordination mode for this sort of ligands implying formal donation of 1 and 3 electrons to the metal atoms, and characterized by an exocyclic M–P distance longer than the endocyclic one. The cycloaddition product of diazomethane is stabilized by a 1,3-shift of a methylenic H atom which yields a phosphanyl intermediate displaying a flat MoPC(H)NN(H) metallacycle with extensive π-delocalization over the C–N–N chain. The reversibility of this H-shift, which is unprecedented, allows for the eventual transformation of this intermediate into the corresponding phosphaethylene derivative, after denitrogenation. The specific formation of P–C bonds in the reactions of **1** with diazoalkanes is in full contrast with the behavior of all other phosphinidene complexes studied to date, either mononuclear or binuclear, which invariably yield products derived from the initial formation of P–N bonds. The

origin of this difference can be traced back to the asymmetric trigonal coordination mode (type **E**) of the phosphinidene ligand in **1**, a view to be corroborated by further investigations on this reactive class of binuclear phosphinidene complexes.

Experimental Section

General Procedures and Starting Materials. All manipulations and reactions were carried out under an argon (99.995%) atmosphere using standard Schlenk techniques. All experiments were carried out using Schlenk tubes equipped with Young´s valves. Solvents were purified according to literature procedures and distilled prior to use.[31] Petroleum ether refers to that fraction distilling in the range 338-343 K. Compound $[Mo_2Cp(\mu\text{-}\kappa^1\text{:}\kappa^1,\eta^5\text{-}PC_5H_4)(CO)_2(\eta^6\text{-}HMes^*)]$ (**1**) (Mes* = 2,4,6-$C_6H_2{}^tBu_3$) was prepared following the improved procedure recently implemented by us,[22] and N_2CPh_2,[32] and Et_2O solutions of N_2CH_2,[33] were prepared as described previously, while all other reagents were obtained from the usual commercial suppliers and used as received, unless otherwise stated. Chromatographic separations were carried out using jacketed columns cooled by tap water (ca. 288 K) or by a closed 2-propanol circuit, kept at the desired temperature with a cryostat. Commercial aluminum oxide (activity I, 70-290 mesh) was degassed under vacuum prior to use. The latter was mixed under argon with the appropriate amount of water to reach activity IV. IR stretching frequencies were measured in solution and are referred to as ν(solvent) and given in wave numbers (cm^{-1}). Nuclear magnetic resonance (NMR) spectra were routinely recorded at 400.13 (^1H), 162.12 ($^{31}P\{^1H\}$), or 100.62 MHz ($^{13}C\{^1H\}$) at 290 K unless otherwise stated. Chemical shifts (δ) are given in ppm, relative to internal tetramethylsilane (^1H, ^{13}C) or external 85% aqueous H_3PO_4 (^{31}P). Coupling constants (J) are given in Hz.

Preparation of $[Mo_2Cp\{\mu\text{-}\kappa^2_{P,S}\text{:}\kappa^1_{S'},\eta^5\text{-}P(CS_2)C_5H_4\}(CO)_2(\eta^6\text{-}HMes^*)]$ (2). Neat CS_2 (4 μL, 0.066 mmol) was added to a toluene solution (2 mL) of compound **1** (0.020 g, 0.031 mmol) and the mixture was stirred at room temperature for 4 h to give a purple solution. The solvent was then removed under vacuum and the residue was chromatographed on alumina at 263 K. Elution with dichloromethane/petroleum ether (1/1) gave a purple fraction yielding, upon removal of solvents, compound **2** as a red-brown microcrystalline solid (0.019 g, 85%). The crystals used in the X-ray diffraction study were grown through the slow diffusion of a layer of petroleum ether into a concentrated dichloromethane solution of the complex at 253 K. Anal. Calcd for $C_{31}H_{39}Mo_2O_2PS_2$: C, 50.96; H, 5.38; S, 8.78. Found: C, 51.21; H, 5.36; S, 8.71. ^1H NMR (C_6D_6): δ 5.88 (m, 1H, C_5H_4), 5.24 (m, 1H, C_5H_4), 5.00 (s, 5H, Cp), 4.71 (s, 3H, C_6H_3), 3.92 (m, 1H, C_5H_4), 3.41 (m, 1H, C_5H_4), 1.06 (s, 27H, ^tBu). $^{13}C\{^1H\}$ NMR (C_6D_6): δ 250.6 (s, MoCO), 250.3 (d, J_{CP} = 58, PCS_2), 248.7 (d, J_{CP} = 9, MoCO), 105.2 [d, J_{CP} = 46, $C^1(C_5H_4)$], 103.3 [s, $C(C_6H_3)$], 102.6 [d, J_{CP} = 7, $CH(C_5H_4)$], 93.3 (s, Cp),

91.8 [d, J_{CP} = 32, CH(C_5H_4)], 87.3 [s, CH(C_5H_4)], 78.9 [s, CH(C_6H_3)], 75.3 [d, J_{CP} = 6, CH(C_5H_4)], 34.5 [s, C^1(^{t}Bu)], 31.7 [s, C^2(^{t}Bu)].

Preparation of [$Mo_2Cp\{\mu$-$\kappa^2_{P,S}$:κ^1_P,η^5-P(C(NPh)S)C_5H_4}$(CO)_2$(η^6-HMes*)] (3). Neat SCNPh (8 μL, 0.066 mmol) was added to a toluene solution (2 mL) of compound **1** (0.020 g, 0.031 mmol) and the mixture was stirred at room temperature for 15 h to give a green solution. The solvent was then removed under vacuum and the residue was chromatographed on alumina at 263 K. Elution with dichloromethane/petroleum ether (1/5) gave a green fraction yielding, upon removal of solvents, compound **3** as a green microcrystalline solid (0.018 g, 75%). The crystals used in the X-ray diffraction study were grown from a concentrated petroleum ether solution of the complex at 277 K. Anal. Calcd for $C_{37}H_{44}Mo_2NO_2SP$: C, 56.28; H, 5.62; N, 1.77; S, 4.06. Found: C, 55.92; H, 5.07; N, 1.91; S, 3.61. ^{1}H NMR (C_6D_6): δ 7.66 (false d, J_{HH} = 7.5, 2H, Ph), 7.30 (false t, J_{HH} = 7.5, 2H, Ph), 6.98 (t, J_{HH} = 7.5, 1H, Ph), 6.23 (m, 1H, C_5H_4), 5.00 (s, 5H, Cp), 4.95 (s, 3H, C_6H_3), 4.87, 4.61, 4.17 (3m, 3 x 1H, C_5H_4), 1.15 (s, 27H, ^{t}Bu). ^{13}C{^{1}H} NMR (C_6D_6): δ 255.4 (d, J_{CP} = 30, MoCO), 243.0 (s, MoCO), 190.7 (d, J_{CP} = 7, SCN), 148.4 [d, J_{CP} = 21, C^1(Ph)], 128.9, 123.1 [2s, CH(Ph)], 124.4 [s, C^4(Ph)], 112.1 [s, C(C_6H_3)], 95.5 [d, J_{CP} = 37, C^1(C_5H_4)], 93.6 (s, Cp), 89.0 [s, CH(C_5H_4)], 86.7 [d, J_{CP} = 7, CH(C_5H_4)], 85.7 [s, CH(C_5H_4)], 80.1 [d, J_{CP} = 14, CH(C_5H_4)], 71.6 [s, CH(C_6H_3)], 34.9 [s, C^1(^{t}Bu)], 31.3 [s, C^2(^{t}Bu)].

Preparation of [$Mo_2Cp\{\mu$-$\kappa^2_{P,N}$:κ^1_P,η^5-P(CHN_2H)C_5H_4}$(CO)_2$(η^6-HMes*)] (4). An excess of an ethereal solution of N_2CH_2 (ca. 1 mL) was added to a dichloromethane solution (3 mL) of compound **1** (0.045 g, 0.069 mmol) at 203 K, whereby the mixture turned brown instantaneously. The solvent was then removed under vacuum and the residue was chromatographed on alumina at 263 K. Elution with dichloromethane/petroleum ether (1/8) gave a minor brown fraction yielding, after removal of solvents, trace amounts of compound [$Mo_2Cp\{\mu$-η^2:κ^1_P,η^5-P(CH_2)C_5H_4}$(CO)_2$(η^6-HMes*)] (**5a**) as a brown powder. Elution with dichloromethane gave a greenish fraction yielding analogously compound **4** as a brown, thermally unstable powder (0.035 g, 73%). ^{1}H NMR (toluene-d_8, 233 K): δ 6.38 (d, J_{HP} = 32, 1H, PCH), 6.26 (br, 1H, NH), 5.03 (m, 1H, C_5H_4), 4.75 (s, 5H, Cp), 4.72 (d, J_{HP} = 3, 3H, C_6H_3), 4.64, 4.63, 4.23, (3m, 3 x 1H, C_5H_4), 1.05 (s, 27H, ^{t}Bu). ^{13}C{^{1}H} NMR (toluene-d_8, 233 K): δ 244.8 (s, 2 MoCO), 124.0 (s, br, CH), 109.8 [s, C(C_6H_3)], 93.5 (s, Cp), 88.6 [d, J_{CP} = 8, CH(C_5H_4)], 87.4 [s, CH(C_5H_4)], 83.8 [d, J_{CP} = 60, C^1(C_5H_4)], 83.7 [s, CH(C_5H_4)], 81.1 [d, J_{CP} = 15, CH(C_5H_4)], 70.2 [s, CH(C_6H_3)], 34.9 [s, C^1(^{t}Bu)], 31.0 [s, C^2(^{t}Bu)].

Preparation of [$Mo_2Cp\{\mu$-η^2:κ^1_P,η^5-P(CH_2)C_5H_4}$(CO)_2$(η^6-HMes*)] (5a). An excess of an ethereal solution of N_2CH_2 (ca. 1 mL) was added to a dichloromethane solution (3 mL) of compound **1** (0.045 g, 0.069 mmol) at 203 K, and the mixture was

then allowed to reach room temperature and further stirred for 30 min to give a brown solution. Workup of the mixture, as described for **4,** yielded compound **5a** as a brown solid (0.030 g, 65%). In solution, this complex exists as an equilibrium mixture of *syn* and *anti* isomers (see Scheme 4), with the *syn*/*anti* ratio being ca. 1/2 in toluene-d_8 at 233 K. The crystals used in the X-ray study were grown from a concentrated petroleum ether solution of the complex at 253 K. ^{1}H NMR (CD_2Cl_2): δ 5.70 (m, 1H, C_5H_4), 5.17 (s, 5H, Cp), 5.07 (m, 1H, C_5H_4), 4.72 (s, 3H, C_6H_3), 4.90, 4.35 (2m, 2 x 1H, C_5H_4), 1.25 (s, 27H, ^{t}Bu); the methylene resonances could not be identified in this spectrum. Anal. Calcd for $C_{31}H_{41}Mo_2O_2P$: C, 55.70; H, 6.18. Found: C, 55.36; H, 5.85. *Data for syn*-**5a**: ^{1}H NMR (CD_2Cl_2, 233 K): δ 0.54 (dd, J_{HH} = 12, J_{HP} = 7, 1H, CH_2), –0.26 (dd, J_{HH} = 12, J_{CP} = 7, 1H, CH_2); other resonances could not be unequivocally assigned to this isomer due to broadness. ^{13}C{^{1}H} NMR (CD_2Cl_2, 233 K): δ 108.2 [s, C(C_6H_3)], 90.0 [s, Cp], 73.8 [s, CH(C_6H_3)], 33.9 [s, C^1(^{t}Bu)], 31.1 [s, C^2(^{t}Bu)], –27.1 (d, J_{CP} = 39, PCH_2); other resonances could not be unequivocally assigned to this isomer. *Data for anti*-**5a**: ^{1}H NMR (CD_2Cl_2, 233K): δ 0.28 (dd, J_{HH} = 12, J_{HP} = 7, CH_2), 0.10 (dd, J_{HH} = 12, J_{HP} = 7, CH_2); other resonances could not be unequivocally assigned to this isomer due to broadness. ^{13}C{^{1}H} NMR (CD_2Cl_2, 233 K): δ 243.6, 243.2 (2s, br, MoCO), 105.5 [s, C(C_6H_3)], 90.2 (s, Cp), 76.0 [s, CH(C_6H_3)], 33.7 [s, C^1(^{t}Bu)], 31.2 [s, C^2(^{t}Bu)], –29.1 (d, ^1J(C,P) = 32; PCH_2); other resonances could not be unequivocally assigned to this isomer.

Preparation of [$Mo_2Cp\{\mu$-η^2:κ^1_P,η^5-P(CPh_2)C_5H_4}(CO)$_2$(η^6-HMes*)] (5b). A solution of compound **1** (0.023 g, 0.035 mmol) in dichloromethane (3 mL) was mixed at room temperature with a 0.079 M diethyl ether solution of N_2CPh_2 (1 mL, 0.079 mmol). The solvents were then removed under vacuum to give a green-brown residue which was chromatographed on alumina at 288 K. Elution with dichloromethane/petroleum ether (1/4) gave a green fraction yielding, after removal of solvents, compound **5b** as a green powder (0.025 g, 86%). The crystals used in the X-ray study were grown by the slow diffusion of layers of petroleum ether and toluene into a dichloromethane solution of the complex at 253 K. Anal. Calcd for $C_{43}H_{49}Mo_2O_2P$: C, 62.93; H, 6.02. Found: C, 62.55; H, 5.80. ^{1}H NMR (CD_2Cl_2): δ 7.22-6.83 (m, 10H, Ph), 4.97 (m, 1H, C_5H_4), 4.93 (s, 5H, Cp), 4.90 (d, J_{HP} = 5, 3H, C_6H_3), 4.87, 4.80, 3.66 (3m, 3 x 1H, C_5H_4), 1.25 (s, 27H, ^{t}Bu). ^{13}C{^{1}H} NMR (CD_2Cl_2): δ 250.7 (s, MoCO), 243.5 (d, J_{CP} = 15, MoCO), 153.1 [d, J_{CP} = 11, C^1(Ph)], 150.9 [d, J_{CP} = 4, C^1(Ph)], 132.7 [s, C^2(Ph)], 129.4 [d, J_{CP} = 12, C^2(Ph)], 128.3 [d, J_{CP} = 25, P*C*Ph_2)], 127.3, 127.0 [2s, C^3(Ph)], 123.2, 123.1 [2s, C^4(Ph)], 107.2 [s, C(C_6H_3)], 93.9 (s, Cp), 90.1 [d, J_{CP} = 12, C^1(C_5H_4)], 88.4 [d, J_{CP} = 9, CH(C_5H_4)], 86.7 [d, J_{CP} = 4, CH(C_5H_4)], 83.7 [s, CH(C_5H_4)], 82.6 [d, J_{CP} = 16, CH(C_5H_4)], 75.3 [s, CH(C_6H_3)], 34.5 [s, C^1(^{t}Bu)], 31.9 [s, C^2(^{t}Bu)].

Preparation of [$Mo_2Cp\{\mu$-η^2:κ^1_P,η^5-$P(CHSiMe_3)C_5H_4\}(CO)_2(\eta^6$-HMes*)] (5c). Compound **1** (0.023 g, 0.035 mmol) and $N_2CH(SiMe_3)$ (35 μL of a 2 M solution in hexane, 0.070 mmol) were stirred in dichloromethane (3 mL) at room temperature for 2.5 h to give a yellow-brown solution. The solvent was then removed under vacuum and the residue was chromatographed on alumina at 288 K. Elution with dichloromethane/petroleum ether (1/2) gave a yellow-brown fraction yielding, after removal of solvents, compound **5c** as a red-yellow powder (0.020 g, 77 %). In solution, this complex exists as an equilibrium mixture of *syn* and *anti* isomers (see Scheme 4), with the *syn*/*anti* ratio being ca. 2/3 in CD_2Cl_2 at 233 K. Anal. Calcd for $C_{34}H_{49}Mo_2O_2PSi$: C, 55.13; H, 6.67. Found: C, 54.85; H 6.79. *Data for syn*-**5c**: ^{1}H NMR (CD_2Cl_2, 233 K): δ 5.31 (s, 5H, Cp), 5.21, 5.11, 4.85 (3m, 3 x 1H, C_5H_4), 4.99 (d, J_{HP} = 6, 3H, C_6H_3), 4.43 (m, 1H, C_5H_4), 1.17 (s, 27H, ^{t}Bu), 0.04 (s, 9H, $SiMe_3$), –0.66 (d, J_{HP} = 3, 1H, PCH). $^{13}C\{^1H\}$ NMR (CD_2Cl_2, 233 K): δ 108.0 [s, $C(C_6H_3)$], 90.4 (s, Cp), 75.3 [s, $CH(C_6H_3)$], 33.1 [s, $C^1(^tBu)$], 32.0 [s, $C^2(^tBu)$], 2.5 (s, $SiMe_3$), –17.1 (d, J_{CP} = 40, PCH). ^{13}C NMR (CD_2Cl_2, 233 K): δ –17.1 (dd, J_{CH} = 134, J_{CP} = 40, CH). *Data for anti*-**5c**: ^{1}H NMR (CD_2Cl_2, 233 K): δ 5.28 (s, 5H, Cp), 5.25, 5.16 (2m, 2 x 1H, C_5H_4), 4.83 (m, 2H, C_5H_4), 4.72 (d, J_{HP} = 5, 3H, C_6H_3), 1.19 (s, 27H, ^{t}Bu), 0.03 (s, 9H, $SiMe_3$), –0.45 (d, J_{HP} = 6, 1H, PCH). $^{13}C\{^1H\}$ NMR (CD_2Cl_2, 233 K): δ 105.8 [s, $C(C_6H_3)$], 91.3 (s, Cp), 77.0 [s, $CH(C_6H_3)$], 33.9 [s, $C^1(^tBu)$], 32.2 [s, $C^2(^tBu)$], 2.2 (s, $SiMe_3$), –28.3 (d, J_{CP} = 40, CH); other resonances could not be assigned individually to each of the isomers: 246.9-243.7 [4m, MoCO], 90.3 [d, J_{CP} = 8, $CH(C_5H_4)$], 89.0 [d, J_{CP} = 5, $CH(C_5H_4)$], 84.3 [d, J_{CP} = 12, $CH(C_5H_4)$], 83.8 [d, J_{CP} = 15, $CH(C_5H_4)$], 89.5, 88.0, 87.2, 87.0 [4s, $CH(C_5H_4)$]; besides this, the $C^1(C_5H_4)$ resonances could not be even identified in the spectrum. ^{13}C NMR (CD_2Cl_2, 233 K): δ –28.3 (dd, J_{CH} = 134, J_{CP} = 40, CH).

X-ray Structure Determination of Compound 5a. Data were collected on a Smart-CCD-1000 Bruker diffractometer using graphite-monochromated Mo K_α radiation at 120 K. Cell dimensions and orientation matrixes were initially determined from least-squares refinements on reflections measured in 3 sets of 30 exposures collected in 3 different ω regions and eventually refined against all reflections. The software SMART[34] was used for collecting frames of data, indexing reflections, and determining lattice parameters. The collected frames were then processed for integration by the software SAINT,[34] and a multi-scan absorption correction was applied with SADABS.[35] Using the program suite WINGX,[36] the structure was solved by Patterson interpretation and phase expansion using SHELXL2014,[37] and refined with full-matrix least squares on F^2 using SHELXL2014. All non-hydrogen atoms were refined anisotropically, except for C(11), which had to be refined anisotropically in combination with the

instructions DELU and SIMU. All hydrogen atoms were geometrically placed and refined using a riding model.

X-ray Structure Determination of Compounds 5b and 3. Data collection for these compounds was performed at 100 K (**5b**) or 153 K (**3**) on an Oxford Diffraction Xcalibur Nova single crystal diffractometer, using Cu K_α radiation. Images were collected at a 65 mm (62 mm for **3**) fixed crystal-detector distance, using the oscillation method, with 1º oscillation (1.2º for **3**) and variable exposure time per image. Data collection strategy was calculated with the program *CrysAlis Pro CCD*,[38] and data reduction and cell refinement was performed with the program *CrysAlis Pro RED*.[38] An empirical absorption correction was applied using the SCALE3 ABSPACK algorithm as implemented in the latter program. Structure solution and refinements were generally carried out as described for **5a**. Compound **5b** crystallized with half a toluene molecule disordered over two positions related by the symmetry operation –x, –y+1, –z, satisfactorily refined with 0.5 occupancy factors, and the cyclopentadienyl group was also disordered over two sites satisfactorily refined with occupancy factors 0.6/04; these carbon atoms were refined isotropically to prevent their temperature factors from becoming non-positive definite.

X-ray Structure Determination of Compound 2. Data were collected on a Kappa-Appex-II Bruker diffractometer using graphite-monochromated Mo K_α radiation at 100 K. The software APEX[39] was used for collecting frames with the ω/ϕ scans measurement method. The SAINT software was used for data reduction, and a multi-scan absorption correction was applied with SADABS. Structure solution and refinements were carried out as described for **5a**.

Computational Details. All DFT computations were carried out using the GAUSSIAN09 package,[40] in which the hybrid method B3LYP was used with the Becke three-parameter exchange functional[41] and the Lee-Yang-Parr correlation functional.[42] An accurate numerical integration grid (99,590) was used for all the calculations via the keyword Int=Ultrafine. Effective core potentials and their associated double-ζ LANL2DZ basis set were used for the metal atoms.[43] The light elements (P, O, C and H) were described with the 6-31G* basis.[44] Geometry optimizations were performed under no symmetry restrictions, and frequency analyses were performed for all the stationary points to ensure that minimum structures with no imaginary frequencies were achieved.

Supporting Information. A CIF file containing full crystallographic data for compounds **2**, **3**, **5a**, and **5b** (CCDC 1497447-1497450) and a PDF file containing the complete reference 40 and results of DFT calculations (drawings, atomic coordinates and energies) for compound **4** and related species. This material is available free of charge via the Internet at http://pubs.acs.org.

Author Information. Corresponding authors: E-mail: garciame@uniovi.es (M. E. G.), mara@uniovi.es (M. A. R).

Acknowledgment. We thank the Universidad de Oviedo for a grant (to I.A.), the Gobierno del Principado de Asturias for a grant (to I.G.A.) and financial support (Project GRUPIN14-011), the MINECO of Spain for financial support (Project CTQ2012-33187), and the CénitS of Extremadura for access to computing facilities.

Table 5. Crystal Data for New Compounds.

	2	**3**	**5a**	**5b**·1/2C_7H_8
mol formula	$C_{31}H_{39}Mo_2O_2PS_2$	$C_{37}H_{44}Mo_2NO_2PS$	$C_{31}H_{41}Mo_2O_2P$	$C_{93}H_{106}Mo_4O_4P_2$ (2 **5b**·C_7H_8)
mol wt	730.59	789.64	668.49	1733.48
cryst syst	triclinic	triclinic	tetragonal	triclinic
space group	*P* –1	*P* –1	*I*–4	*P* –1
radiation (λ, Å)	0.71073	1.54184	0.71073	1.54184
a, Å	9.6565(5)	10.5874(6)	23.854(2)	9.5101(5)
b, Å	10.4953(6)	11.1625(7)	23.854(2)	12.8133(7)
c, Å	15.7123(9)	15.7439(9)	10.4011(18)	17.9238(7)
α, deg	90.569(4)	95.834(5)	90	103.176(4)
β, deg	102.965(4)	106.289(5)	90	91.152(4)
γ, deg	101.380(4)	95.765(5)	90	109.283(5)
V, Å^3	1518.85(15)	1760.43(19)	5918.6(14)	1996.47(18)
Z	2	2	8	1
calcd density, g cm^{-3}	1.597	1.49	1.50	1.44
absorp coeff, mm^{-1}	1.043	7.065	0.927	5.801
temperature, K	100.0(1)	153(1)	120(2)	100(2)
θ range (deg)	1.33-30.51	2.95-68.68	1.71-26.46	2.55-73.82
index ranges (*h*, *k*, *l*)	–13, 13; –14, 14; –22, 22	–12, 12; –13, 13; –18, 18	–29, 29; –29, 29; –13, 12	–11, 11; –14, 15; –22, 17
no. of reflns collected	68043	15400	24204	20633
no. of indep reflns (R_{int})	9273 (0.0467)	6488 (0.0365)	6091 (0.0965)	7536 (0.0619)
no. of reflns with $I > 2\sigma(I)$	7730	5914	4465	5704
R indexes [data with $I > 2\sigma(I)$][a]	R_1 = 0.0275 wR_2 = 0.0551[b]	R_1 = 0.0345 wR_2 = 0.0893[c]	R_1 = 0.0506 wR_2 = 0.0866[d]	R_1 = 0.0529 wR_2 = 0.1473[e]
R indexes (all data)[a]	R_1 = 0.0378 wR_2 = 0.0599[b]	R_1 = 0.0379 wR_2 = 0.093[c]	R_1 = 0.083 wR_2 = 0.0964[d]	R_1 = 0.0747 wR_2 = 0.1579[e]
GOF	1.041	1.015	1.032	1.052
no. of restraints/parameters	0 / 312	0 / 406	15 / 334	0 / 471
$\Delta\rho$(max., min.), eÅ^{-3}	0.588, –0.467	0.709 / –1.022	0.807, –0.684	1.159, –1.578
CCDC deposition No	1497447	1497448	1497449	1497450

[a] $R = \Sigma||F_o| - |F_c|| / \Sigma|F_o|$. $wR = [\Sigma w(|F_o|^2 - |F_c|^2)^2 / \Sigma w|F_o|^2]^{1/2}$. $w = 1/[\sigma^2(F_o^2) + (aP)^2 + bP]$ where $P = (F_o^2 + 2F_c^2)/3$. [b] a = 0.0223, b = 0.9971. [c] a = 0.0581, b = 0.6192. [d] a = 0.0174, b = 41.3682. [e] a = 0.0527, b = 19. 5816.

References

1. (a) Wit, J. B. M.; de Jong, G. B.; Schakel, M.; Lutz, M.; Ehlers, A. W.; Slootweg, J. C.; Lammertsma, K. *i*Pr_2N–P=$Fe(CO)_4$ in olefinic solvents: A reservoir of a Transient Phosphinidene Complex Capable of Substrate Hoping. *Organometallics* **2016**, *35*, 1170-1176. (b) Wong, J.; Hao, Y.; Tian, R.; Mathey, F. Isomerization of Secondary Phosphirane into Terminal Phosphinidene Complexes: An Analogy between Monovalent Phosphorus and Transition Metals. *Angew. Chem. Int. Ed.*

2015, *54*, 12891-12893. (c) Lv, Y.; Kefalidis, C. E.; Zhou, J.; Maron, L.; Leng, X.; Chen, Y. Versatile reactivity of a four-coordinate scandium phosphinidene complex: reduction, addition, and CO activation reactions. *J. Am. Chem. Soc.* **2013**, *135*, 14784-14796. (d) Waterman, R.; Tilley, T. D. Terminal hafnium phosphinidene complexes and phosphinidene ligand exchange. *Chem. Sci.* **2011**, *2*, 1320-1325.

2. Recent reviews: (a) Mathey, F.; Duan, Z. Activation of A–H bonds (A = B, C, N, O, Si) by using monovalent phosphorus complexes [RP→M]. *Dalton Trans.* **2016**, *45*, 1804-1809. (b) Aktas, H.; Slootweg, J. C.; Lammertsma, K. Nucleophilic phosphinidene complexes: access and applicability. *Angew. Chem. Int. Ed.* **2010**, *49*, 2102-2113. (c) Waterman, R. Metal-phosphido and -phosphinidene complexes in P–E bond-forming reactions. *Dalton Trans.* **2009**, 18-26. (d) Mathey, F. Developing the chemistry of monovalent phosphorus. *Dalton Trans.* **2007**, 1861-1868. (e) Lammertsma, K. Phosphinidenes. *Top. Curr. Chem.* **2003**, *229*, 95-119. (f) Lammertsma, K.; Vlaar, M. J. M. Lammertsma, K. & Vlaar, M. J. M. Carbene-Like Chemistry of Phosphinidene Complexes − Reactions, Applications, and Mechanistic Insights. *Eur. J. Org. Chem.* **2002**, 1127-1138. (g) Streubel, R. Chemistry of λ^3-2*H*-azaphosphirene metal complexes. *Coord. Chem. Rev.* **2002**, *227*, 175-192. (h) Mathey, F.; Tran Huy, N. H.; Marinetti, A. Electrophilic Terminal-Phosphinidene Complexes: Versatile Phosphorus Analogues of Singlet Carbenes. *Helv. Chim. Acta* **2001**, *84*, 2938-2957. (i) Stephan, D. W. Zirconium – Phosphorus Chemistry: Strategies in Syntheses, Reactivity, Catalysis, and Utility. *Angew. Chem. Int. Ed.* **2000**, *39*, 314–329. (j) Shah, S.; Protasiewicz, J. D. 'Phospha-variations' on the themes of Staudinger and Wittig: phosphorus analogs of Wittig reagents. *Coord. Chem. Rev.* **2000**, *210*, 181-201.

3. Dillon, K. B.; Mathey, F.; Nixon, J. F. *Phosphorus: The Carbon-Copy*; Wiley: Chichester, 1998, p. 19.

4. (a) Alvarez, C. M.; Alvarez, M. A.; García, M. E.; González, R.; Ruiz, M. A.; Hamidov, H.; Jeffery, J. C. High-yield Synthesis and Reactivity of Stable Diiron Complexes with Bent-Phosphinidene Bridges. *Organometallics* **2005**, *24*, 5503-5505. (b) Alvarez, M. A.; García, M. E.; González, R.; Ruiz, M. A. Nucleophilic and Electrophilic Behavior of the Phosphinidene-Bridged Complex $[Fe_2(\eta^5\text{-}C_5H_5)_2(\mu\text{-}PCy)(\mu\text{-}CO)(CO)_2]$. *Organometallics* **2008**, *27*, 1037-1040. (c) Alvarez, M. A.; García, M. E.; González, R.; Ruiz, M. A. Reactions of the Phosphinidene-Bridged Complexes $[Fe_2(\eta^5\text{-}C_5H_5)_2(\mu\text{-}PR)(\mu\text{-}CO)(CO)_2]$ (R = Cy, Ph, 2,4,6-$C_6H_2{}^tBu_3$) with Diazoalkanes. Formation and Rearrangements of Phosphadiazadiene-Bridged Derivatives. *Organometallics* **2010**, *29*, 5140-5153. (d) Alvarez, M. A.; García, M. E.; González, R.; Ruiz, M. A. Reactions of the

Phosphinidene-Bridged Complexes $[Fe_2(\eta^5\text{-}C_5H_5)_2(\mu\text{-}PR)(\mu\text{-}CO)(CO)_2]$ (R = Cy, Ph) with Electrophiles Based on p-Block Elements. *Dalton Trans* **2012**, *417*, 14498-14513. (e) Alvarez, M. A.; García, M. E.; González, R.; Ruiz, M. A. P−C and C−C Coupling Processes in the Reactions of the Phosphinidene-Bridged Complex $[Fe_2(\eta^5\text{-}C_5H_5)_2(\mu\text{-}PCy)(\mu\text{-}CO)(CO)_2]$ with Alkynes. *Organometallics* **2013**, *32*, 4601-4611.

5. Albuerne, I. G.; Alvarez, M. A.; García, M. E.; García-Vivó, D.; Ruiz, M. A. Novel Dimerization of Maleic Anhydride at a Mo_2 Complex: Phase-Driven Keto/Enol Tautomerism in a Phosphinidenium-Ylide Complex. *Organometallics* **2013**, *32*, 6178-6181.
6. (a) Schiffer, M.; Scheer, M. On the pathway of the η^1–η^5 migration of a Cp* ligand. *J. Chem. Soc., Dalton Trans.* **2000**, 2493-2494. (b) Schiffer, M.; Scheer, M. Trapping Reactions of an Intermediate Containing a Tungsten–Phosphorus Triple Bond with Alkynes. *Chem. Eur. J.* **2001**, *7*, 1855-1861. (c) Schiffer, M.; Scheer, M. Insertion Reactions of Nitriles into the P−C Bond of $[(\eta^1\text{-}C_5Me_5)P\{W(CO)_5\}_2]$-A Novel Approach to Phosphorus-Containing Heterocycles. *Angew. Chem. Int. Ed.* **2001**, *40*, 3413-3416. (d) Scheer, M.; Himmel, D.; Johnson, B. P.; Kuntz, C.; Schiffer, M. Ring expansion of a Cp* moiety: formation of a 1,2-diphosphacyclooctatetraene ligand. *Angew. Chem. Int. Ed. Engl.* **2007**, *46*, 3971-3975. (e) Seidl, M.; Schiffer, M.; Bodensteiner, M.; Timoshkin, A. Y.; Scheer, M. Reactivity of Bridged Pentelidene Complexes with Isonitriles: A New Way to Pentel-Containing Heterocycles. *Chem. Eur. J.* **2013**, *19*, 13783-13791. (f) Seidl, M.; Kuntz, C.; Bodensteiner, M.; Timoshkin, A. Y.; Scheer, M. Reaction of Tungsten–Phosphinidene and –Arsinidene Complexes with Carbodiimides and Alkyl Azides: A Straightforward Way to Four-Membered Heterocycles. *Angew. Chem. Int. Ed.* **2015**, *54*, 2771-2775. (g) Seidl, M.; Weinzierl, R.; Timoshkin, A. Y.; Sheer, M. Insight into the Reaction of a Dinuclear Phosphinidene Complex with Nitriles. *Chem. Eur. J.* **2016**, *22*, 5484-5488. (h) Seidl, M.; Balázs, G.; Timoshkin, A. Y.; Scheer, M. Stepwise Formation of a 1,3-Butadiene Analogue of Mixed Heavier Group 15 Elements. *Angew. Chem. Int. Ed.* **2016**, *55*, 431-435.
7. Graham, T. W.; Udachin, K. A.; Carty, A. J. Reactivity of electrophilic μ-phosphinidene complexes with heterocumulenes: formation of the first σ-π-aminophosphaimine complexes $[Mn_2(CO)_8\{\mu\text{-}\eta^1,\eta^2\text{-}P(NiPr_2)=NR\}]$ and diazoalkane insertions into metal-phosphorus bonds. *Chem. Commun.* **2005**, 4441-4443.
8. (a) Cui, P.; Chen, Y.; Xu, X.; Sun, J. An unprecedented lanthanide phosphinidene halide: synthesis, structure and reactivity. *Chem. Commun.* **2008**, 5547-5549. (b) Masuda, J. D.; Jantunen, K. C.; Ozerov, O. V.; Noonan, K. J. T.; Gates, D. P.;

Scott, B. L.; Kiplinger, J. L. A Lanthanide Phosphinidene Complex: Synthesis, Structure, and Phospha-Wittig Reactivity. *J. Am. Chem. Soc.* **2008**, *130*, 2408-2409.

9. (a) Alvarez, M. A.; Amor, I.; García, M. E.; García-Vivó, D.; Ruiz, M. A. Carbene- and Carbyne-like Behavior of the Mo–P Multiple Bond in a Dimolybdenum Complex Inducing Trigonal Pyramidal Coordination of a Phosphinidene Ligand. *Inorg. Chem.* **2007**, *46*, 6230-6232. (b) Alvarez, M. A.; García, M. E.; Ruiz, M. A.; Suárez, J. Enhanced Nucleophilic Behaviour of a Dimolybdenum Phosphinidene Complex: Multicomponent Reactions with Activated Alkenes and Alkynes in the Presence of CO or CNXyl. *Angew. Chem. Int. Ed.* **2011**, *50*, 6383-6387. (c) Alvarez, M. A.; Amor, I.; García, M. E.; García-Vivó, D.; Ruiz, M. A.; Suárez, J. Reactivity of the Phosphinidene-Bridged Complexes $[Mo_2Cp(\mu\text{-}\kappa^1\text{:}\kappa^1,\eta^5\text{-}PC_5H_4)(\eta^6\text{-}1,3,5\text{-}C_6H_3{}^tBu_3)(CO)_2]$ and $[Mo_2Cp_2(\mu\text{-}PH)(\eta^6\text{-}1,3,5\text{-}C_6H_3{}^tBu_3)(CO)_2]$ Toward Alkynes: Multicomponent Reactions in the Presence of Ligands. *Organometallics* **2012**, *31*, 2749-2763.
10. (a) Malisch, W.; Grün, K.; Fey, O.; Abd El Baky, C. [2+2]-Cycloaddukte PH-funktioneller Phosphenium-Komplexe mit Alkylisothiocyanaten: Darstellung von $C_5R_5(OC)_2M\text{–}P(H)(t\text{-}Bu)\text{–}C(=NR')\text{–}S$ (R=H, Me; M=Mo, W; R′=Me, Et, *t*-Bu) und Reaktion unter Beanspruchung der PH-Funktion: Phosphenium-Übergangsmetallkomplexe, 37. *J. Organomet. Chem.* **2000**, *595*, 285-291. (b) Malisch, W.; Abd El Baky, C.; Grün, K.; Reising, J. Reaction of the Phosphenium Complexes $Cp(OC)_2W\text{-}P(t\text{Bu})(R)$ with Ethyl Isothiocyanate: Unprecedented Fornmation of the Phosphametalla Spiro Compound $\{Cp(OC)_2W\text{–}P(t\text{Bu})(R)\text{–}N(Et)\text{–}C^a[N(Et)\text{–}(CH)\text{–}N(Et)C^bH_2]\text{–}S(W\text{–}S)(C^a\text{–}C^b)\}Cl$ (R = *t*Bu, Ph). *Eur. J. Inorg. Chem.* **1998**, 1945-1949. (c) Pfister, H.; Malisch, W. Cycloadditionsreaktionen von phospheniumkomplexen: VIII. Regioselektive cycloaddition chiraler phosphenium-komplexe $Cp(OC)[Ph_2(R)P]M{=}PPh_2$ (M = Mo, W; R = H, Me) mit isothiocyanaten. *J. Organomet. Chem.* **1992**, *439*, C11-C15.
11. Antiñolo, A.; García-Yuste, S.; Otero, A.; Reguillo-Carmona, R. Insertion Reactions of Isothiocyanates into the Nb–P Bond of Phosphide-Niobiocene Complexes. *Eur. J. Inorg. Chem.* **2009**, 539-544.
12. Cordero, B.; Gómez, V.; Platero-Prats, A. E.; Revés, M.; Echevarría, J.; Cremades, E.; Barragán, F.; Alvarez, S. Covalent radii revisited. *Dalton Trans.* **2008**, 2832-2838.
13. Pyykkö, P.; Atsumi, M. Molecular Double-Bond Covalent Radii for Elements Li-E112. *Chem. Eur. J.* **2009**, *15*, 12770-12779.
14. Galindo, A.; Miguel, D.; Perez, J. Phosphine-carbon disulfide adducts, S_2CPR_3: versatile ligands in coordination chemistry. *Coord. Chem. Rev.* **1999**, *193-195*, 643-690.

15. Amor, I.; García, M. E.; Ruiz, M. A.; Sáez, D.; Hamidov, H.; Jeffery, J. C. Formation and Cleavage of P–C, Mo–C, and C–H Bonds Involving Arylphosphinidene and Cyclopentadienyl Ligands at Dimolybdenum Centers. *Organometallics* **2006**, *25*, 4857-4869.
16. Rosenberg, L. Metal Complexes of Planar PR_2 Ligands: Examining the Carbene Analogy. *Coord. Chem. Rev.* **2012**, *256*, 606-626.
17. Malisch, W.; Maisch, R.; Colquhoun, I. J.; McFarlane, W. Übergangsmetall-substituierte phosphane, arsane und stibane: XXVIII. Übergangsmetall-diphenylphosphane von molybdän und wolfram; darstellung, reaktionen und NMR-spektroskopische charakterisierung. *J. Organomet. Chem.* **1981**, *220*, C1-C6.
18. Weber, L.; Uthmann, S.; Bogge, H.; Muller, A.; Stammler, H.-G.; Neumann, B. Synthesis, Structure, and Coordination Chemistry of P-Acyl, P-Thiocarbamoyl and P-Dithiocarboxyl-Substituted Phosphaalkenes $R(X)C–P=C(NMe_2)_2$ (R= Ph, *t*Bu, $SSiMe_3$, $N(Ph)SiMe_3$; X= O, S). *Organometallics* **1998**, *17*, 3593-3598.
19. Alvarez, B.; Alvarez, M. A.; Amor, I.; García, M. E.; García-Vivó, D.; Ruiz, M. A.; Suárez, J. Dimolybdenum Cyclopentadienyl Complexes with Bridging Chalcogenophosphinidene Ligands. *Inorg. Chem.* **2012**, *51*, 7810-7824.
20. Alvarez, M. A.; Amor, I.; García, M. E.; García-Vivó, D.; Ruiz, M. A.; Suárez, J. Structure, Bonding and Reactivity of Binuclear Complexes having Asymmetric Trigonal Phosphinidene Bridges: Addition of 16-electron Metal Carbonyl Fragments to the Dimolybdenum Compounds $[Mo_2Cp(\mu\text{-}\kappa^1\text{:}\kappa^1,\eta^5\text{-}PC_5H_4)(CO)_2L]$ and $[Mo_2Cp_2(\mu\text{-}PH)(CO)_2L]$ (L = η^6-1,3,5-$C_6H_3{}^tBu_3$). *Organometallics.* **2010**, *29*, 4384-4395.
21. Carty, A. J.; MacLaughlin, S. A.; Nucciarone, D. in *Phosphorus- 31 NMR Spectroscopy in Stereochemical Analysis*; Verkade, J. G., Quin, L. D., Eds.; VCH: Deerfield Beach, FL, 1987; Chapter 16.
22. Albuerne, I. G.; Alvarez, M. A.; García, M. E.; García-Vivó, D.; Ruiz, M. A. Electronic Structure and Multisite Basicity of the Pyramidal Phosphinidene-Bridged Dimolybdenum Complex $[Mo_2(\eta^5\text{-}C_5H_5)(\mu\text{-}\kappa^1\text{:}\kappa^1,\eta^5\text{-}PC_5H_4)(\eta^6\text{-}C_6H_3tBu_3)(CO)_2(PMe_3)]$. *Inorg. Chem.* **2015**, *54*, 9810-9820.
23. Graham, T. W.; Udachin, K. A.; Carty, A. J. Reactivity patterns of thermally stable, terminal, electrophilic phosphinidene complexes towards diazoalkanes: oxidation at the phosphorus centre and formation of P-bound η^1-phosphaazine, η^1-phosphaalkene and η^3-diazaphosphaallene complexes. *Chem. Commun.* **2005**, 5890-5892.
24. Graham, T. W.; Udachin, K. A.; Zgierski, M. Z.; Carty, A. J. Synthesis and Structural Characterization of the First Thermally Stable, Neutral, and Electrophilic Phosphinidene Complexes of Vanadium. *Organometallics* **2011**, *30*, 1382-1388.

25. Weber, L. Recent developments in the chemistry of metallophosphaalkenes. *Coord. Chem. Rev.* **2005**, *249*, 741-763.
26. (a) Apfel, R.; Casser, C.; Knoch, F. Über niederkoordinierte phosphorverbindungen: XXXX. 2,4,6-tri-t-Butylphenylmethylenphosphan,ein vielseitiger ligand in übergangsmetall-komplexen. *J. Organomet. Chem.* **1985**, *293*, 213-217. (b) Davies, J. E.; Mays, M. J.; Raithby, P. R.; Woods, A. D. Reactivity of acryloyl chloride towards the anion $[Cp_2(CO)_4Mo_2(\mu\text{-}PPhH)]^-$; synthesis of an unusual phosphaalkene. *Chem. Commun.* **1999**, 2455-2456. (c) Brym, M.; Jones, C.; Waugh, M.; Hey-Hawkins, E.; Majoumo, F. Reactions of phosphavinyl Grignard reagents with aldehydes: synthesis, characterisation and further reactivity of β-phosphaallylic alcohols. *New J. Chem.* **2003**, *27*, 1614-1621.
27. P. S. Braterman, *Metal Carbonyl Spectra*; Academic Press: London, U. K., 1975.
28. (a) Dartiguenave, M.; Menu, M. J.; Deydier, E.; Dartiguenave, Y.; Siebald, H. Crystal and molecular structures of transition metal complexes with N- and C-bonded diazoalkane ligands. *Coord. Chem. Rev.* **1998**, *178-180*, 623-663. (b) Mizobe, Y.; Ishii, Y.; Hidai, M. Synthesis and reactivities of diazoalkane complexes. *Coord. Chem. Rev.* **1995**, *139*, 281-311.
29. Malisch, W.; Grün, K.; Fried, A.; Reich, W.; Pfister, H.; Huttner, G.; Zsolnai, L. Cycloadditionsreaktionen von Molybdän- und Wolfram-Phospheniumkomplexen mit Diazoethylacetat: Synthese und strukturelle Charakterisierung von drei- und fünf-gliedrigen Phosphametallacyclen: Phosphenium-Komplexe, 39. *J. Organomet. Chem.* **1998**, *566*, 271-276.
30. Chan, T. L.; Xie, Z. The synthesis, structure and reactivity of an imine-stabilized carboranylphosphorus(I) compound. *Chem. Commun.* **2016**, *52*, 7280-7283.
31. Armarego, W. L. F.; Chai, C. *Purification of Laboratory Chemicals, 7th ed.*; Butterworth-Heinemann: Oxford, U. K, 2012.
32. Miller, J. B. Preparation of Crystalline Diphenyldiazomethane. *J. Org. Chem.* **1959**, *24*, 560-561.
33. Vogel, A. I. *Textbook of Practical Organic Chemistry, 4th ed.*; Longmans: London, U. K., 1978, p 291.
34. *SMART & SAINT Software Reference Manuals, Version 5.051*; Bruker Analytical X-ray Instruments: Madison WI, 1998.
35. Sheldrick, G. M. *SADABS, Program for Empirical Absorption Correction*; University of Göttingen: Göttingen, Germany, 1996.
36. Farrugia, L. J. WinGX suite for small-molecule single-crystal crystallography. *J. Appl. Crystallogr.* **1999**, *32*, 837-838.
37. Sheldrick, G. M. A short history of SHELX. *Acta Crystallogr.* **2008**, *A64*, 112-122.
38. *CrysAlis Pro*; Oxford Diffraction Limited, Ltd.: Oxford, U. K., 2006.

39. *APEX 2, version 2.0-1*, Bruker AXS Inc: Madison, WI, 2005.
40. Frisch, M. J. et al., *Gaussian 09, Revision D.01*, see the Supporting Information for the complete reference.
41. Becke, A. D. Density-functional thermochemistry. III. The role of exact exchange. *J. Chem. Phys.* **1993**, *98*, 5648-5652.
42. Lee, C.; Yang, W.; Parr, R. G. Development of the Colle-Salvetti correlation-energy formula into a functional of the electron density. *Phys. Rev. B* **1988**, *37*, 785-789.
43. Hay, P. J.; Wadt, W. R. Ab initio effective core potentials for molecular calculations. Potentials for potassium to gold including the outermost core orbitals. *J. Chem. Phys.* **1985**, *82*, 299-310.
44. (a) Hariharan, P. C.; Pople, J. A. Influence of polarization functions on MO hydrogenation energies. *Theor. Chim. Acta* **1973**, *28*, 213-222. (b) Petersson, G. A.; Al-Laham, M. A. A complete basis set model chemistry. II. Open-shell systems and the total energies of the first-row atoms. *J. Chem. Phys.* **1991**, *94*, 6081-6090. (c) Petersson, G. A.; Bennett, A.; Tensfeldt, T. G.; Al-Laham, M. A.; Shirley, W. A.; Mantzaris, J. A complete basis set model chemistry. I. The total energies of closed-shell atoms and hydrides of the first-row elements. *J. Chem. Phys.* **1988**, *89*, 2193.-2218.

(For Table of Contents Use Only)

Table of Contents Synopsis

All starts at the metal site! The title complex undergoes different cycloaddition reactions with several heterocumulenes, but the process is initiated in all cases by heteroatom coordination of the cumulene to the metal site, this triggering a P–C bond formation step *via* nucleophilic attack of the phosphinidene P atom.

Graphics for Table of Contents